Combined Atomic Force Microscopy–Fluorescence Microscopy: Analyzing Exocytosis in Alveolar Type II Cells

ARTICLE *in* ANALYTICAL CHEMISTRY · JUNE 2012

Impact Factor: 5.64 · DOI: 10.1021/ac300775j · Source: PubMed

7 AUTHORS, INCLUDING:

Elena Hecht
Universität Ulm
9 PUBLICATIONS **66** CITATIONS
SEE PROFILE

Manfred Frick
Universität Ulm
55 PUBLICATIONS **944** CITATIONS
SEE PROFILE

Paul Dietl
Universität Ulm
84 PUBLICATIONS **1,404** CITATIONS
SEE PROFILE

Christine Kranz
Universität Ulm
130 PUBLICATIONS **2,448** CITATIONS
SEE PROFILE

analytical chemistry

Article

pubs.acs.org/ac

Combined Atomic Force Microscopy–Fluorescence Microscopy: Analyzing Exocytosis in Alveolar Type II Cells

Elena Hecht,[†] Kristin Thompson,[‡] Manfred Frick,*[,‡] Oliver H. Wittekindt,[‡] Paul Dietl,[‡] Boris Mizaikoff,[†] and Christine Kranz*[,†]

[†]Institute of Analytical and Bioanalytical Chemistry, University of Ulm, Albert-Einstein-Allee 11, 89081 Ulm, Germany

[‡]Institute of General Physiology, University of Ulm, Albert-Einstein-Allee 11, 89081 Ulm, Germany

Supporting Information

ABSTRACT: Hybrid atomic force microscopy (AFM)–fluorescence microscopy (FM) investigation of exocytosis in lung epithelial cells (ATII cells) allows the detection of individual exocytic events by FM, which can be simultaneously correlated to structural changes in individual cells by AFM. Exocytosis of lamellar bodies (LBs) represents a slow form of exocytosis found in many non-neuronal cells. Exocytosis of LBs, following stimulation with adenosine-5′-triphosphate (ATP) and phorbol 12-myristate 13-acetate (PMA), results in a cation influx via $P2X_4$ receptors at the site of LB fusion with the plasma membrane (PM), which should induce a temporary increase in cell height/volume. AFM measurements were performed in single-line scans across the cell surface. Five minutes after stimulation, ATII cells revealed a cell height and volume increase of 13.7% ± 4.1% and 15.9 ± 4.8% (N = 9), respectively. These transient changes depend on exocytic LB–PM fusion. Nonstimulated cells and cells lacking LB fusions did not show a significant change in cell height/volume (N = 8). In addition, a cell height decrease was observed in ATII cells stimulated by uridine-5′-triphosphate (UTP) and PMA, agonists inducing LB fusion with the PM, but not activation of $P2X_4$ receptors. The cell height and volume decreased by −8.6 ± 3.6% and −11.2 ± 3.9% (N = 5), respectively. Additionally, low force contact and dynamic mode AFM imaging of cell areas around the nucleus after stimulation with ATP/PMA was performed. Fused LBs are more pronounced in AFM topography images compared to nonfused LBs, concluding that different "dynamic states" of LBs or locations from the PM are captured during imaging.

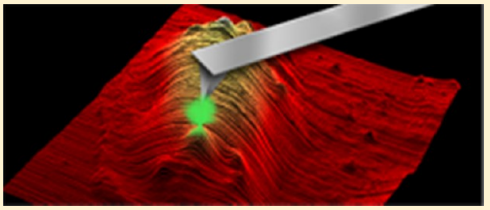

Atomic force microscopy (AFM) has evolved into an indispensable analytical tool, in particular in combination with fluorescence microscopy for studying biological samples such as proteins, nucleotides, membranes, and living cells. Information on biomolecular structures with submolecular resolution may be obtained under physiological conditions.[1] For example, AFM has been used to investigate the activity of single protein structures in vitro during signaling events. The possibility to measure elasticity changes of a secretory cell in real-time may provide information on the cortical cytoskeleton during exocytosis.[2] Recently, it was shown that AFM is suitable for investigating chemically induced endocytosis in fixed and living alveolar type II (ATII) cells, which is characterized by a substrate uptake from the outer medium into the cell.[3] In this study, a decrease in cell surface roughness and cell height associated with endocytosis was observed. Moreover, combining AFM with optical techniques such as fluorescence microscopy (FM) provides further detailed information on cellular processes and enables enhanced visualization of cells and subcellular structures, for example, by fluorescence-labeled membrane proteins and molecules[4] or labeled elements of the cytoskeleton,[5] or secretory vesicle contents.[6] Especially, the investigation of exocytosis, the fusion of secretory vesicles with the plasma membrane (PM), which is usually accompanied by release of the vesicle content and a morphological change of the cell surface, is of particular interest. AFM studies investigating the mechanism of such exocytic processes have been reported, focusing on imaging of depression structures that are related to the formation of fusion pores in pancreatic acinar cells[7,8] and in neuroendocrine cells.[9] Typically, exocytosis of neurotransmitters occurs on a time scale of milliseconds,[10] whereas the exocytic release of macromolecular complexes is a comparatively slow process, which occurs within seconds[11] to minutes.[7] ATII cells represent such "slow secreters".[12]

The alveolar epithelium with ATI and ATII cells plays a significant role in surfactant secretion, regulation of alveolar fluid homeostasis, and maintenance of the gas–blood barrier between the alveolar space and the pulmonary capillaries. ATI cells are the primary sites for gas exchange, but both cell types (ATI and ATII cells) are involved in maintaining alveolar function. It has been shown that the mechanosensitive release of ATP by ATI cells serves as a paracrine stimulator for surfactant secretion in ATII cells.[13] ATII cells release pulmonary surfactant (PS), a phospholipid-rich lipoprotein-like substance, via exocytosis of lamellar bodies (LBs). LBs are large storage organelles with a diameter of 1–5 μm.[14] Upon release of PS into the alveolar hypophase, PS reduces the surface tension at the air–liquid interphase and prevents

Received: April 3, 2012
Accepted: June 11, 2012
Published: June 12, 2012

   dx.doi.org/10.1021/ac300775j | *Anal. Chem.* 2012, 84, 5716–5722

alveolae from collapsing. The overall exocytic response to stimulation occurs over a period of approximately 20 min.[15] Thus, the time scale of regulated exocytosis in ATII cells is comparable to the time resolution of AFM imaging experiments, allowing the structural and functional characterization of LB fusion and release of PS. The dynamic of the release from surfactant-containing LBs is the subject of extensive ongoing research;[16−18] for example, Haller et al. studied the dynamics of surfactant release with FM.[19] Until now, there is little information about morphology changes of the cell surface during exocytosis in ATII cells, which involves fusion of the LB with the PM. Extracellular ATP has been known for some time to be a potent secretagogue that stimulates the fusion of LBs and/or release of PS in ATII cells.[20] Recently, Miklavc et al. reported that stimulation of ATII cells with ATP also leads to a localized, "fusion-activated" Ca^{2+}-entry at the site of LB fusion in primary ATII cells.[21] This Ca^{2+}-entry is mediated via $P2X_4$ receptors expressed on LBs of ATII cells that are inserted in the cell surface upon exocytic fusion of LBs with the PM.[12] It is likely that this fusion-dependent cation influx also leads to changes in cell volumes. The recovery of the original state in ATII cells that involves special regulatory volume mechanisms such as the Na−K-pump was investigated by Jones et al.[22] In contrast to ATP, extracellular UTP also causes LB fusion with the PM, however does not lead to fusion-dependent inward currents.[12]

A standard method for volume measurements is the Coulter counter, which is used to determine size and shape of cells in suspension, e.g., blood cells[23] or bacteria.[24] In contrast, AFM enables in vitro imaging of adherent life cells, resulting in information on surface structures and cell dynamics in buffered solutions. AFM is also highly suitable for the investigation of cell morphology and volume changes induced by chemical or mechanical stimulation applied to the cell environment.[7,25,26] In these AFM studies, the whole cells were imaged; however, to capture cell height/area changes with sufficient time resolution, line scans instead of complete images may be performed by moving the AFM tip back and forth at the same y position and recording z height changes as a function of time. As the AFM tip may penetrate soft cellular material,[27,28] minimization of the force exerted by the AFM tip to the cell surface is a prerequisite during such studies. Operation at low forces (i.e., <5 nN) results in significantly reduced cell compression or damage.

The fusion process of LBs with the PM in ATII cells is described as a process with two main phases, the prefusion and postfusion phase.[20] During the prefusion phase, LBs approach the PM and, via a hemifusion intermediate stage, fuse with the PM, which leads to an opening of the fusion pore. During the postfusion phase, release of surfactant into the extracellular space is tightly controlled by fusion pore dynamics and active expulsion mechanisms ("kiss-coat and release"). Ultimately, most LBs collapse into the PM. In addition, some LBs can fuse with the PM but remain in the PM without further dynamics ("kiss-coat and wait mechanism"). Coating of LBs with the PM as well as the retraction back into the cell is tightly associated with F-actin.[29]

Here, we present AFM in combination with fluorescence microscopy as a bioanalytical tool to study cell height/area changes while inducing exocytosis in ATII cells at physiological conditions. Combined AFM-FM studies facilitate the correlation of cell height changes (AFM topographical data) with fluorescence data labeling the sites of exocytic events or visualization of LB fusion with the PM. AFM measurements recorded in low force contact[30] and/or dynamic mode with loading forces between 0.5 and 5 nN result in undistorted cell images. During AFM measurements, a series of frames of FM images were captured. Furthermore, the capability of AFM for imaging different "states" of LBs correlating with nonprefused as well as fused LBs was investigated. The obtained results indicate that AFM combined with FM provides new insight into exocytic processes and cell volume regulation at a single cell level and hence renders the combination highly suitable for bioanalytical research.

EXPERIMENTAL SECTION

Cell Isolation and Cultivation. ATII cells were isolated from male Sprague−Dawley rats according to the method of Dobbs et al.[31] with minor modifications as previously described.[21] After isolation, cells were seeded on glass coverslips, cultured in MucilAir (Epithelix, Switzerland) at 37 °C and 5% CO_2, and used for experiments for up to 48 h after isolation.

Experimental Conditions for Stimulation with ATP (UTP)/PMA. All experiments were performed in bath solution (BS in mM: 140 NaCl, 5 KCl, 1 $MgCl_2$, 2 $CaCl_2$, 5 glucose, 10 HEPES; pH 7.4). Dye FM 1−43 (1 μM) was added to the BS prior to the experiments (typical concentration: 1 μM), as FM 1−43 is nonfluorescent in BS. ATII cells were stimulated with ATP or UTP (final concentration: 30 μM) and PMA (300 nM). The reported concentrations of ATP/PMA and UTP/PMA were adapted to the optimal concentration for inducing LB fusion and surfactant secretion.[32]

FM Imaging of Fusion Events and Image Analysis. Fusion events in the investigated cells were visualized using dye FM 1−43, as described in detail elsewhere.[19,33] FM 1−43 was excited at 488 nm using a Visichrome High Speed polychromator system (Visichrome, Germany). For measurement of FM 1−43 fluorescence, cells were illuminated for 150 ms. Bright field (BF) and fluorescence images were recorded with a LCPlanFI-Olympus 40×/0.6 objective and an EZ CCD-camera (excitation 488 nm, GFP-filter, and emission of 500−540 nm). Data acquisition was facilitated by Metamorph software version 7.5.5.0 (Visitron Systems GmbH, Puchheim, Germany). FM images were analyzed using ImageJ software.

Atomic Force Microscopy. A model 5500 atomic force microscope from Agilent Technologies, (Chandler, AZ) was used. For combined measurements, the atomic force microscope was mounted on an IX81, Olympus inverted microscope. A V-shaped silicon nitride cantilever with a nominal spring constant of 0.06 N/m (Bruker, Camarillo, CA) was used. While scanning across the cell surface, we directly added ATP/PMA or UTP/PMA to the AFM cell. Images were recorded with a resolution of 512 × 512 pixels. AFM studies of fused and nonfused LBs were recorded in low force contact and dynamic mode (drive frequency 38 kHz, damping of the amplitude of 20%, if not otherwise stated), respectively.

Data Analysis of AFM Images. For cell height/area studies, AFM topography data were analyzed with Pico View (Chandler, AZ) software (Version 1.8.4) using a first-order algorithm correcting for piezo-derived differences between line scans. Cross sections were collected from images directly after stimulation to identify cell height/area changes due to fluctuations. Reported area changes reflect the area under the cross-section curve as shown in the Supporting Information (Figure S1). Consecutively, cross sections were derived at

dx.doi.org/10.1021/ac300775j | Anal. Chem. 2012, 84, 5716−5722

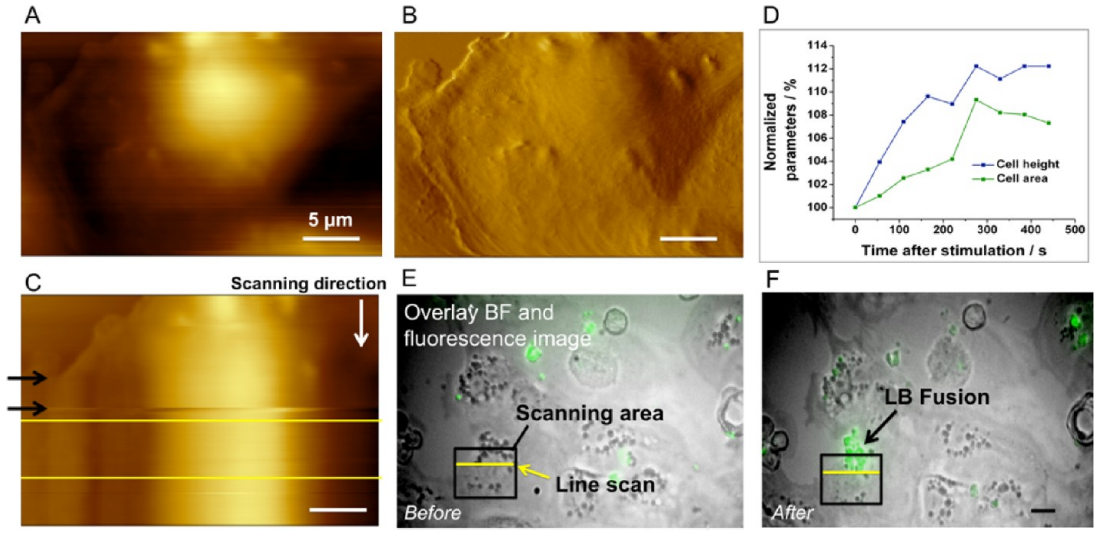

Figure 1. (A) Low force contact mode AFM topography image and (B) deflection image of a live ATII cell before stimulation (rectangle: 37 × 18 µm, scan speed: 0.23 ln/s, scan direction: bottom to top). (C) Topography image of the time study (same cell as shown in A and B, respectively). Switching from rectangular scan to line scan (marked with an arrow), followed by treatment with ATP/PMA (marked with an arrow; after treatment, line scans were performed for approximately 8 min). Yellow lines mark times when cross sections are taken. (D) The analysis of profile extractions taken at different times. An overlay of the bright field image and the fluorescence image before and after treatment and AFM imaging is shown in E and F, respectively. The rectangle reflects the AFM scan area, and the yellow line shows the site where line scans were started. LB fusion results in a fluorescence signal after treatment (green spots in G in the area of the AFM scan).

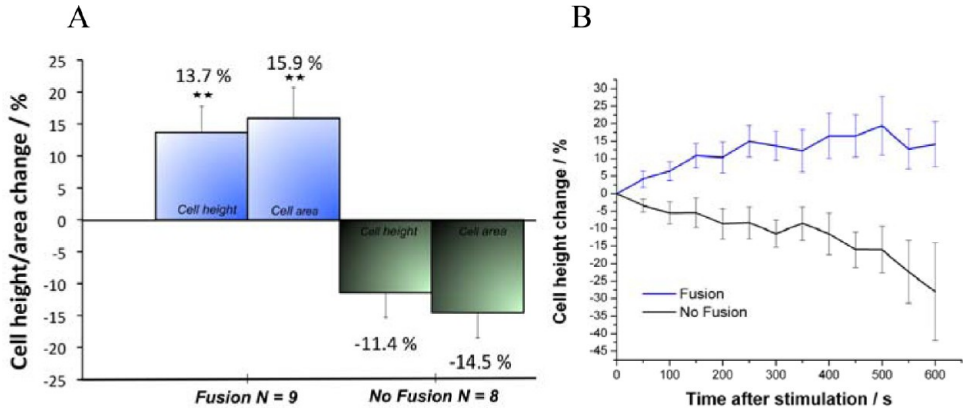

Figure 2. Profile extraction after stimulation. (A) Data 300 s after stimulation show an increase in cell height of 13.7% ± 4.1% and cell area of 15.9 ± 4.8% when fusion occurred (N = 9) and a cell height/area decrease of −11.4 ± 3.9% and −14.5 ± 4.0% when no fusion occurred (no fluorescence signals after AFM imaging and stimulation, N = 8). (B) Cell height change over time of all investigated cells when ATP-stimulated fusion took place (blue line (N = 9)) and when no fusion occurred (black line (N = 8)).

different times after stimulation (every 40 s, if not noted otherwise).

Statistical Analysis. Data are presented as mean value ± standard error of the mean value (SEM). To verify statistical significance, an unpaired two-tailed Student's t test was applied. Differences were considered statistical significant at a $p < 0.05$ level and are indicated with double asterisk.

RESULTS AND DISCUSSION

Cell Volume Increase Due to Stimulation with ATP/PMA. AFM measurements of cell height/volume as well as morphology changes were recorded after stimulation with ATP(UTP)/PMA in real-time. Figure 1 shows the AFM topography (A) and deflection (B) image of an ATII cell recorded in low force contact mode (calculated force of 5 nN; see Supporting Information for force calculation). LBs besides the cell nucleus were not fused, as no fluorescence signal is visible in the FM image (Figure 1E) before ATP/PMA stimulation. Hence, such cells with no fused LBs are highly suitable for the conducted studies, as the probability to induce an exocytic response by stimulating with ATP/PMA is high.[20] Initially, a rectangle is scanned until the y axis is disabled (marked with an arrow in Figure 1C). After performing a line scan for a given time (for this particular experiment, 250 s), we stimulated the cells with ATP/PMA (again marked with an arrow), while scanning in the x direction is continued for approximately 8 min. Cross sections taken directly after stimulation and at selected times after stimulation reveal a remarkable increase in cell height and area within the reported time (Figure 1D). The analysis of the profile extractions (yellow line in 1C) directly and 5 min after stimulation shows an increase in cell height (maximal height of the profile extraction) of 9% and area under the profile extraction curve of 11%. It is assumed that the cell swells due to fusion-induced

dx.doi.org/10.1021/ac300775j | Anal. Chem. 2012, 84, 5716−5722

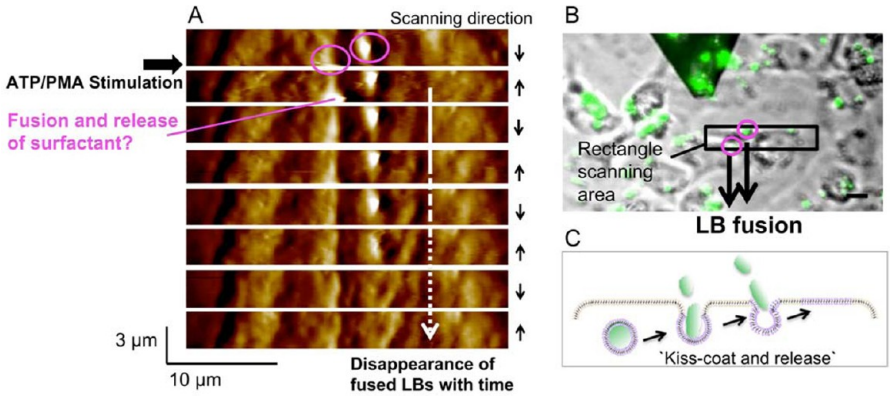

Figure 3. AFM images recorded while simultaneously stimulating ATII cells with ATP/PMA. Low force contact mode AFM deflection images (A) of the time series. The scan speed was 0.30 ln/s (calculated force: 4 nN). Recording one image took approximately 1 min. LBs visible as bumps in the AFM deflection images (marked with a magenta circle) disappear within minutes after ATP/PMA stimulation. (B) Optical images show an overlay of the bright field with the fluorescence image after stimulation and after AFM imaging. Two fluorescence spots are visible (marked with a circle in the scanned area), indicating that fusion occurred, and probably correspond to the LBs, which are imaged by AFM. (C) Scheme of the postulated fusion mechanism.

influx of ions and consequently influx of water. LB fusion in the investigated cell was confirmed by correlative FM images. The FM image (Figure 1F recorded after stimulation and AFM imaging) reveals that a fluorescence signal is observed in the investigated cell. In addition, the obtained data suggest that an exocytic event affects the entire cell, as cell swelling is not only observed at the site where LBs fuse with the PM. In this particular example, approximately five fusion events occurred in the investigated cell, which had a cell size of approximately 25 μm. The LB diameter is on the order of 1−3 μm; hence, it may be expected that such fusion not only causes a local change, at the site of LBs, but also causes an alteration of the entire cell.

AFM line scan experiments were performed 17 times (different dishes) while the cells were stimulated with ATP/PMA (as shown in Figure 2B); in nine cases, LBs fused in the examined cell, and consecutive cell swelling was observed, documented by an increase in cell height of 13.7 ± 4.1% (N = 9) as well as an increase in cell area of 15.9 ± 4.8% (N = 9) measured 5 min after stimulation. In contrast, if no LB fusion occurred (N = 8), the cell height decreased (N = 6) or remained almost constant (N = 2). The average values of all data when no fusion took place are in the range of −11.4 ± 3.9% (decrease in cell height) and −14.5 ± 4.0% (decrease in cell area). These differences in cell height/area vary between cells that show LB fusion and between cells without exocytic events after stimulation with ATP/PMA. Student's t test was applied for unpaired samples; the difference between the increase in cell height and area for observed LB fusion is significant toward data when no fusion was observed. In Figure 2A, Student's t test, $p < 0.05$, is indicated by stars in the diagram.

Control Experiments Investigating Changes in Cell Height Due to Force Interaction. On average, the cells were scanned for a period of 12 min. Hence, the cell height/area decrease in the case where no fusion was observed may be related either to the force interaction of the AFM tip with the cell surface or changes in the osmolality of the bath solution given the duration of the experiments. Changes in cell height due to changes in the bath solution were also observed in confocal microscopy studies of ATII cells (unpublished results). Although the force interaction is significantly reduced when operating in low force contact mode[30] or dynamic mode, the force impediment of the AFM tip, which cannot be entirely omitted,[34] may have an effect on the obtained cell heights. Hence, control experiments were conducted, adding only BS to the fluid cell (N = 5). These experiments resulted in a decrease in cell height (−5.2 ± 2.8%) and cell area (−8.8 ± 3.1%) approximately 5 min after administering BS (shown in Figure S2C). However, none of the control experiments led to an increase in cell height. Therefore, an increase in cell height and cell area, respectively, after LB fusion was induced with ATP/PMA is a clear indication for an influx of ions and water into the cell, leading to the observed cell swelling.

In addition, in cells with fusion events (increase in cell height), after approximately 9 min, the cell height was restored to basal levels in most cases (N = 6) (see Supporting Information Figure S2A). A decrease in cell height of 9% and in cell area of 10% was observed after the initial swelling. Exemplarily, such data are shown in Figure S2B (Supporting Information). The cell adapts to alterations in volume with regulatory mechanisms such as ion transport across the cell membrane or metabolic processes,[35] which is necessary for maintaining normal cellular homeostasis. Secretion of lung surfactant is a highly regulated process,[36] and recovery of the original state is probably an indicator for the health of ATII cells. Additionally, no fluorescence signals were observed after 12 min of AFM scanning, which is an indication that the cells are not damaged during the experiments.

Stimulation with UTP/PMA. Both ATP and UTP activate primarily $P2Y_2$ at the surface of ATII cells receptors,[18] whereas PMA activates the protein kinase C (PKC) cascade.[37] ATP and UTP stimulate fusion but only ATP, and not UTP, activates $P2X_4$ receptors,[38] and therefore UTP does not cause a fusion-activated influx of ions in ATII cells.[12] To support this hypothesis, the cell height studies were repeated, stimulating with UTP instead of ATP (N = 5) (data presented in the Supporting Information Figure S3A−C). Similar to ATP, fusion was induced but, in contrast, no cell height increase was observed when stimulating with UTP. Upon analysis of the obtained height profiles, a decrease in cell height, as shown in Figure 3S, of −7% 5 min after stimulation (mean cell height change −8.6 ± 3.6%, N = 5) and a decrease in cell area of −10% 8 min after stimulation (mean cell area change −11.2 ± 3.9%, N = 5) were observed. LB fusion with the PM occurred in

dx.doi.org/10.1021/ac300775j | Anal. Chem. 2012, 84, 5716−5722

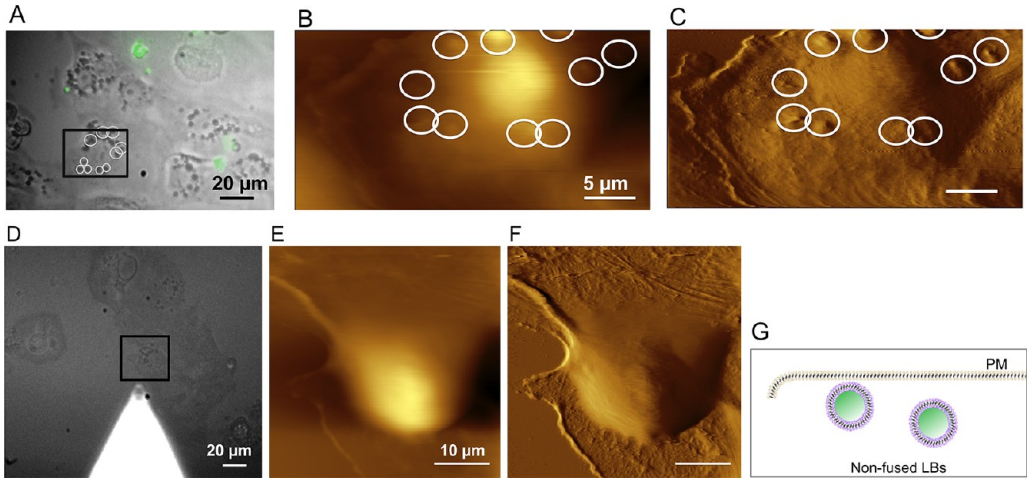

Figure 4. (A) Overlay of the bright field and fluorescence image prior to AFM imaging. Green spots indicate prefused LBs. Nonprefused LBs inside the AFM scanning area (rectangle) are denoted with a white circle. (B) AFM topography and (C) deflection image recorded in low force contact mode (rectangle scan: 38 × 18 μm, scan speed: 0.23 ln/s (calculated force: 3.6 nN). (D) Bright field image of ATII cells with LBs (rectangle indicates the AFM scanning area). (E) AFM topography image and (F) deflection image of the cell shown in D (scan area: 40 × 40 μm, scan speed: 0.44 ln/s, calculated force: 2.1 nN). A schematic of LBs located under the PM without fusion is shown in G.

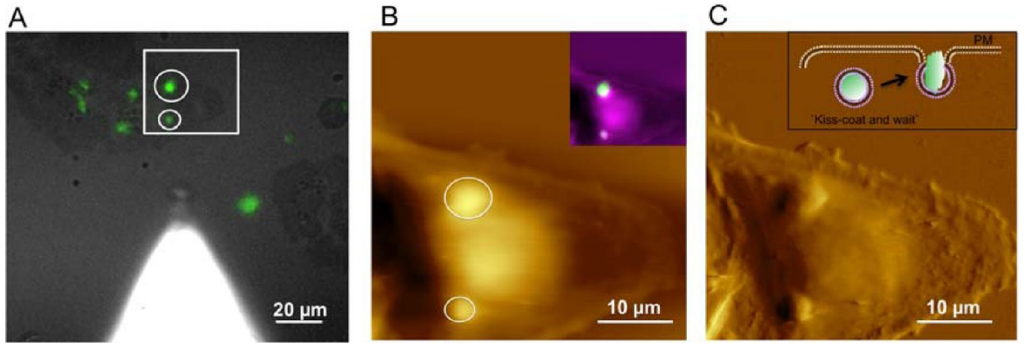

Figure 5. (A) Overlay of the bright field and fluorescence image 15 min after cells were stimulated with UTP/PMA. LB fusion is visible as bright FM 1−43 fluorescence. The AFM scanned area is marked with a square. B: AFM topography image; inset in B shows an overlay of the fluorescence image (green) with the AFM topography (magenta). C: AFM deflection image. Scan area: 40 × 40 μm, scan speed: 0.44 ln/s, calculated force: 1.8 nN. Inset in C shows the schematic of postulated dynamic state of LBs.

the examined cell (visible in corresponding FM images). The cell height decreased 100 s after adding UTP (inset in Figure S3D), and LB fusion occurred approximately 80 s after stimulation; the cell was imaged for approximately 12 min. Similar to the control experiment, stimulation with UTP resulted in a reduction in cell height. Whether this decrease may be related to the activation of Cl^--secretion[39] and water efflux mediated by P2Y receptors or changes in the bath osmolality or force interaction cannot be determined at this point. However, the obtained AFM data reveal that in contrast to ATP, UTP does not activate $P2X_4$ receptors on fused lamellar bodies. Up to now, there is little information on ion transport regulation via UTP in ATII cells, and a variety of mechanisms are proposed in the literature.[40] For examined cells with no fusion events (N = 4), a decrease in cell volume was also observed (for example, cell area change of −11.4 ± 5.5% determined 5 min after stimulation; data not shown).

AFM Imaging of Cell Morphology Changes Due to ATP-Stimulated Exocytosis. Further experiments address morphology changes during the slow process of exocytosis in ATII cells. Two phases, the prefusion and postfusion phases, which are connected by fusion of the secretory vesicle with the PM, should result in different morphology visible in the AFM images. As described by Haller et al.,[41] the postfusion phase may take up to several hours; however, considerable variation between individual LBs was reported. In the prefusion phase, only LBs residing beneath the PM are detected by AFM as regularly shaped, micrometer-sized protrusions.[6] A rectangular area was continuously scanned while the cell was stimulated with ATP/PMA (Figure 3A shows the deflection image of a time series). LBs (marked with a circle in Figure 3A and 3B), which are visible as elevated areas in the AFM topography image, disappear within minutes after stimulation with ATP/PMA. The fusion of these LBs with the PM (Figure 3B shows the FM image of those fusion events as green spots) leads to a comparatively flat area in the AFM image. Flattening of LBs is likely due to stimulated exocytosis of these surface-bound, ready to fuse LBs, which leads to surfactant release and subsequent flattening of the LB membrane into the PM (scheme shown in Figure 3C). The surfactant-containing vesicles under the PM are located besides the cell nucleus and can fuse with the PM and release PS ("kiss-coat and release"[29]) to maintain alveolar tension. Furthermore, the white distorted spot in the second deflection image (Figure 3A left second rectangle) probably represents such an exocytic event where PS was released. The highly viscous lipoprotein-like PS probably

dx.doi.org/10.1021/ac300775j | Anal. Chem. 2012, 84, 5716−5722

sticks to the AFM tip, resulting in the visible distortion. The second LB evident in the AFM deflection image reflects a LB, which appears already fused with the PM (see FM 1−43 staining in Figure 3B) remains static without surfactant release. As shown in the AFM sequence, PS is not released, and it appears that the LB returns under the PM after a certain period (approximately 6 min after fusion) and hence cannot be detected by AFM anymore. This might represent a rare "kiss-coat and run" fusion described by Miklavc et al.[29] Overall, cell morphology changes for LB fusion with the PM could be routinely observed by AFM. If no fusion was observed (absent fluorescence signal), no topographical changes in the AFM images were evident (data not shown). In addition, control experiments where the cell was imaged for a certain time (10−12 min) without stimulation did not yield significant morphology changes (N = 3).

AFM Imaging of "Different States" of LBs. AFM images were recorded for nonprefused LBs and were interpreted with respect to "states" during their fusion with the PM and/or release of PS. If vesicles are nonfused (no fluorescence signal (Figure 4A)), the vesicles mostly appear as small elevations in the AFM image (Figure 4B,C) or are not detected by the AFM tip (Figure 4E,F) if they are not in close vicinity to the PM (Figure 4G). Almost all nonfused LBs shown in Figure 4A (marked with a rectangle) are also evident in the AFM topography (B) and deflection (C) image (marked with a white circle) beside the cell nucleus. An example where LBs are not resolved in the AFM images, although they are visible in the bright field image, is given in Figure 4, parts D (bright field image), E (topography), and F (deflection).

Fused vesicles (green dots in Figure 5A) resulted in more pronounced features in AFM topography (Figure 5B) and deflection (Figure 5C) image, respectively. The overlay of the fluorescence image and AFM topography image (inset in Figure 5B) reveals a perfect fit. For this particular example, it seems that no surfactant is released because the AFM image is not distorted and the imaging conditions were stable over time. After vesicle transport and fusion with the PM, surfactant remains entrapped within the fused vesicles.[42] A schematic of the mechanism involving only LB fusion without further action ("kiss-coat and wait") is shown in the inset of Figure 5C. AFM images were recorded in low force contact (N = 8) as well as dynamic mode (N = 4).

Fusion and release of surfactant, a lipoprotein-rich substance, typically follows docking or priming of LBs to the PM. When the fusion of LBs resulted in surfactant secretion, in most cases (>60% of fused vesicles, N = 8), FM 1−43 labeled surfactant was "pushed away" by the AFM tip (Supporting Information Figure S4).

CONCLUSION

The unique capability of AFM combined with FM as a bioanalytical tool for studying dynamic processes in live cells is demonstrated. AFM/FM allows correlation of topographical changes in live cells with molecular specificities of cell structures, which was demonstrated in the investigation of exocytosis in ATII cells. The synchronized study of cell behavior induced by chemical stimulation provides information on the dynamics as well as on topography changes. Performing AFM line scans, we obtained cell height/volume changes in live cells on a seconds-to-minute time scale in response to external stimuli under physiological conditions. Upon induction of exocytosis in ATII cells using ATP, a cell height/volume increase (initial phase) followed by cell height/volume decrease (second phase) was observed. ATII cells do not reveal an increase in cell height/volume when LB fusion was induced by UTP, thereby supporting the hypothesis of a secretagogue-selective, fusion-dependent pathway for cell volume regulation. Furthermore, imaging parts of a cell around the nucleus while stimulating the cells revealed changes in cell morphology due to LB fusion with the PM. Before stimulation, several LBs were evident as elevated areas in the AFM images, which then disappeared within minutes after stimulation, most likely indicating that they fused with the PM, releasing their contents into the extracellular space and collapsing into the PM.

In conclusion, complementary data simultaneously obtained with AFM and FM enables the correlation of cell morphology changes with molecular pathways of surfactant exocytosis in lung ATII cells including the transport from vesicles to the PM, docking or priming, release of PS, and cell volume regulation mechanisms.

ASSOCIATED CONTENT

Supporting Information

Additional information as noted in the text. This material is available free of charge via the Internet at http://pubs.acs.org.

AUTHOR INFORMATION

Corresponding Author

*(C.K.) E-mail: christine.kranz@uni-ulm.de, phone: (+49) 7315022479, fax: (+49)7315022463; (M.F.) e-mail: manfred.frick@uni-ulm.de, phone: (+49)73150023115, fax: (+49) 73150023242.

Notes

The authors declare no competing financial interest.

ACKNOWLEDGMENTS

T. Felder and M. Timmler are acknowledged for technical assistance, in particular for primary alveolar type II cell isolation.

REFERENCES

(1) Jena, B. P.; Cho, S.-J. *Methods Cell Biol.* **2002**, *68*, 33−50.
(2) Fernandez, J. M. *Proc. Natl. Acad. Sci. U.S.A.* **1997**, *94*, 9−10.
(3) Hecht, E.; Usmani, S. M.; Albrecht, S.; Wittekindt, O. H.; Dietl, P.; Mizaikoff, B.; Kranz, C. *Anal. Bioanal. Chem.* **2011**, *399*, 2369−2378.
(4) Madl, J.; Rhode, S.; Stangl, H.; Stockinger, H.; Hinterdorfer, P.; Schuetz, G. J.; Kada, G. *Ultramicroscopy* **2006**, *106*, 645−651.
(5) Kidoaki, S.; Matsuda, T. *J. Biomed. Mater. Res., Part A* **2007**, *81A*, 803−810.
(6) Miklavc, P.; Hecht, E.; Hobi, N.; Wittekindt, O. H.; Dietl, P.; Kranz, C.; Frick, M. *J. Cell Sci.* **2012**, in press.
(7) Schneider, S. W.; Sritharan, K. C.; Geibel, J. P.; Oberleithner, H.; Jena, B. P. *Proc. Natl. Acad. Sci. U.S.A.* **1997**, *94*, 316−321.
(8) Cho, S.-J.; Wakade, A.; Pappas, G. D.; Jena, B. P. *Ann. N.Y. Acad. Sci.* **2002**, *971*, 254−256.
(9) Tsai, C.-C.; Yang, C.-C.; Shih, P.-Y.; Wu, C.-S.; Chen, C.-D.; Pan, C.-Y.; Chen, Y.-T. *J. Phys. Chem. B* **2008**, *112*, 9165−9173.
(10) Matthews, G. *Annu. Rev. Neurosci.* **1996**, *19*, 219−233.
(11) Klingauf, J.; Kavalali, E. T.; Tsien, R. W. *Nature* **1998**, *394*, 581−585.
(12) Miklavc, P.; Mair, N.; Wittekindt, O. H.; Haller, T.; Dietl, P.; Felder, E.; Timmler, M.; Frick, M. *Proc. Natl. Acad. Sci. U.S.A.* **2011**, *108*, 14503−14508 , S14503/1−S14503/7..
(13) Patel, A. S.; Reigada, D.; Mitchell, C. H.; Bates, S. R.; Margulies, S. S.; Koval, M. *Am. J. Physiol.* **2005**, *289*, L489−L496.

(14) Szallasi, A.; Gronowski, A. M.; Eby, C. S. *Clin. Chem.* **2003**, *49*, 994−997.
(15) Dietl, P.; Liss, B.; Felder, E.; Miklavc, P.; Wirtz, H. *Cell. Physiol. Biochem.* **2010**, *25*, 1−12.
(16) Singer, W.; Frick, M.; Haller, T.; Bernet, S.; Ritsch-Marte, M.; Dietl, P. *Biophys. J.* **2003**, *84*, 1344−1351.
(17) Rose, F.; Kurth-Landwehr, C.; Sibelius, U.; Reuner, K. H.; Aktories, K.; Seeger, W.; Grimminger, F. *Am. J. Respir. Crit. Care Med.* **1999**, *159*, 206−212.
(18) Rice, W. R.; Singleton, F. M. *Br. J. Pharmacol.* **1987**, *91*, 833−838.
(19) Haller, T.; Ortmayr, J.; Friedrich, F.; Völkl, H.; Dietl, P. *Proc. Natl. Acad. Sci. U.S.A.* **1998**, *95*, 1579−1584.
(20) Wemhöner, A.; Frick, M.; Dietl, P.; Jennings, P.; Haller, T. *J. Biomol. Screen.* **2006**, *11*, 286−295.
(21) Miklavc, P.; Frick, M.; Wittekindt, O. H.; Haller, T.; Dietl, P. *PLoS One* **2010**, *5*, e10982.
(22) Jones, G. S.; Miles, P. R.; Lantz, R. C.; Hinton, D. E.; Castranova, V. *J. Appl. Physiol.: Respir., Environ. Exercise Physiol.* **1982**, *53*, 258−266.
(23) Simiele, M.; D'Avolio, A.; Baietto, L.; Siccardi, M.; Sciandra, M.; Agati, S.; Cusato, J.; Bonora, S.; Di Giovanni, P. *Antimicrob. Agents Chemother.* **2011**, *55*, 2976−2978.
(24) Kubitschek, H. E.; Friske, J. A. *J. Bacteriol.* **1986**, *168*, 1466−1467.
(25) Oberleithner, H.; Schneider, S. W.; Albermann, L.; Hillebrand, U.; Ludwig, T.; Riethmueller, C.; Shahin, V.; Schaefer, C.; Schillers, H. *J. Membr. Biol.* **2003**, *196*, 163−172.
(26) Schneider, S. W.; Pagel, P.; Rotsch, C.; Danker, T.; Oberleithner, H.; Radmacher, M.; Schwab, A. *Pfluegers Arch.* **2000**, *439*, 297−303.
(27) Domke, J.; Dannohl, S.; Parak, W. J.; Muller, O.; Aicher, W. K.; Radmacher, M. *Colloids Surf., B* **2000**, *19*, 367−379.
(28) Radmacher, M. *Methods Cell Biol.* **2002**, *68*, 67−90.
(29) Miklavc, P.; Wittekindt, O. H.; Felder, E.; Dietl, P. *Ann. N.Y. Acad. Sci.* **2009**, *1152*, 43−52.
(30) Le Christian, G.; Lesniewska, E.; Giocondi, M.-C.; Finot, E.; Vie, V.; Goudonnet, J.-P. *Biophys. J.* **1998**, *75*, 695−703.
(31) Dobbs, L. G.; Gonzalez, R.; Williams, M. C. *Am. Rev. Respir. Dis.* **1986**, *134*, 141−145.
(32) Frick, M.; Eschertzhuber, S.; Haller, T.; Mair, N.; Dietl, P. *Am. J. Respir. Cell Mol. Biol.* **2001**, *25*, 306−315.
(33) Wirtz, H. R.; Dobbs, L. G. *Science* **1990**, *250*, 1266−1269.
(34) You, H. X.; Yu, L. *Methods Cell Sci.* **1999**, *21*, 1−17.
(35) Lang, F.; Busch, G. L.; Ritter, M.; Volkl, H.; Waldegger, S.; Gulbins, E.; Haussinger, D. *Physiol. Rev.* **1998**, *78*, 247−306.
(36) Chintagari, N. R.; Mishra, A.; Su, L.; Wang, Y.; Ayalew, S.; Hartson, S. D.; Liu, L. *PLoS One* **2010**, *5*, e9228.
(37) Chander, A.; Sen, N.; Wu, A.-M.; Spitzer, A. R. *Am. J. Physiol.* **1995**, *268*, L108−L116.
(38) North, R. A. *J. Biol. Chem.* **2002**, *281*, 15044−15049.
(39) Mall, M.; Wissner, A.; Gonska, T.; Calenborn, D.; Kuehr, J.; Brandis, M.; Kunzelmann, K. *Am. J. Respir. Cell Mol. Biol.* **2000**, *23*, 755−761.
(40) Yang, C.; Su, L.; Wang, Y.; Liu, L. *Am. J. Physiol.* **2009**, *297*, L439−L454.
(41) Haller, T.; Dietl, P.; Pfaller, K.; Frick, M.; Mair, N.; Paulmichl, M.; Hess, M. W.; Furst, J.; Maly, K. *J. Cell Biol.* **2001**, *155*, 279−89.
(42) Dietl, P.; Haller, T. *Annu. Rev. Physiol.* **2005**, *67*, 595−621.